Dynamics of Charging of Muscovite Mica: Measurement and Modeling

Paul J. Sides,* Danish Faruqui, and Andrew J. Gellman

Department of Chemical Engineering, Carnegie Mellon University, Pittsburgh, Pennsylvania 15213

Received August 22, 2008. Revised Manuscript Received November 10, 2008

The advent of a new method for measuring the zeta potential of planar surfaces, the rotating disk, allowed the investigation of the charging process of mica after immersion in water. The zeta potential of freshly cleaved muscovite mica was recorded within seconds of immersion of the sample and in fractions of a second thereafter. The zeta potential of mica in water at pH = 5.6 with no added potassium changed by 40−50 mV over approximately 1 min. A model of adsorption and desorption of potassium ions and protons captured this behavior and provided a framework for determination of surface adsorption rate constants. The charging of mica in alkaline KCl solutions of arbitrary concentration, however, was too fast for observation. The equilibrium zeta potential depended on the logarithm of salt concentration, in agreement with a model based on ion exchange reactions. The average values of the proton adsorption, proton desorption, potassium adsorption, and potassium desorption rate coefficients were 45 L/s ± 15, 0.0014/s ± 0.0006, 58 L/s ± 5, and 0.14/s ± 0.03, respectively. An equation giving the zeta potential as a function of the rate parameters and the concentrations of potassium ions and protons was derived. It is demonstrated that subtraction of zeta potentials, measured at different solution compositions within the same experiment, eliminates extrinsic factors and brings data from disparate measurements into agreement.

Introduction

Zeta potential characterizes the electrical properties of the interfaces of charged surfaces in solution.[1] Solids acquire charge when in contact with solution by ionization of surface groups, differential loss of ions from the crystal lattice, and adsorption of charged species from solution. Conventional uses of zeta potential include characterization of dispersions and prediction of forces between surfaces. Zeta potential is sensitive to the surface concentration of charged species; the zeta potential of a freshly cleaved muscovite mica surface in water having a conductivity of 1 μS/cm varies by 1 mV when the surface fraction of charged sites changes by approximately 0.01%.

Muscovite mica, an important mineral in colloid science, has the fundamental formula $KAl_2(AlSi_3O_{10})(OH)_2$. It is a 2:1 clay mineral; oxygen tetrahedrally coordinates two layers of silicon atoms and octahedrally coordinates one aluminum atom layer for every unit cell. An aluminum atom substitutes for every fourth silicon atom in the tetrahedral layer where the charge balance is $3Si^{4+} + Al^{3+} + 8\ O^{2-} \Rightarrow Si_3AlO_8^{1-}$. Consequently, muscovite mica has a net single negative charge per surface unit cell. Mica is easily cleaved into sheets because each surface unit cell has sites for two potassium atoms, only one of which is necessary to satisfy overall charge neutrality. On cleaving along the basal plane, one-half the potassium ions present in a single layer of an intact crystal remain with one face, and the other half of the potassium ions depart with the other face. Both faces are ionically neutral after separation.

Mica's sheet-forming attribute allows exposure of an atomically smooth and fresh surface by cleaving. Israelachvili and Adams,[2] while measuring forces between mica sheets in a range of aqueous inorganic electrolytes, reported values of the apparent zeta potential of mica deduced as a fitting parameter from their force/distance curves. The values for ruby and green muscovite mica ranged from −50 to −130 mV; the authors speculated that differences in the detailed compositions of different mica types must explain the differing values. Pashley[3,4] reported mica surface potential values ranging from −60 to −165 mV in a variety of solutions of NaCl and HCl, again deduced from force measurements. Shubin and Kekicheff,[5] fitting force curves taken in $LiNO_3$ solutions, found surface potentials of −120 mV at pH 5.7 and salt concentration 1 mM. Raviv et al.[6] investigated the time dependence of normal forces between muscovite mica surfaces in conductivity water and their relation to ion exchange on the surface. Mica surfaces separated after adhesive contact regained their characteristic surface charge density on the time scale of 1 h; hysteresis was recorded in the force measured during this period. They attributed this change in behavior to the effect of co-ions near the surfaces in reducing the effective activation energy for ion release from the mica lattice; quantification of the kinetics of various surface interactions occurring in these experiments, however, was not possible by the technique used.

Zeta Potential from Streaming Potential Measurements. Israelachvili and Adams's[2] finding of an anomalous force between mica surfaces spurred interest in the direct measurement of the zeta potential of mica. Lyons et al.[7] reported zeta potential measurements for mica as a function of time in terms of days. Early transient behavior of the zeta potential was much different from the steady state or equilibrium value. They noted several points about mica surface aging: (i) Aging at pH 10 in silica vessels produced a surface very similar in electrokinetic behavior to a pure silica surface after a number of days, reflecting the deposition of hydrolyzed silicon species onto the mica surface. (ii) Aging at pH 3 produced a surface that, upon pH increase, showed electrokinetic behavior reflecting the adsorption of aqueous aluminum species or other hydrolyzable metal ions from solutions. This was more pronounced for crushed, as distinct from sheet, mica. (iii) Aging at pH 7 was minimal. (iv) Aging at pH 4 was less significant in the presence of aqueous 1:1 metal ions such as potassium. These measurements gave clues about

(1) Hunter, R. *Zeta Potential*; Academic Press: New York, 1981.
(2) Israelachvili, J. N.; Adams, G. E. *J. Chem. Soc., Faraday Trans. 1* **1978**, *74*, 975.
(3) Pashley, R. M. *J. Colloid Interface Sci.* **1981**, *80*, 153.
(4) Pashley, R. M. *J. Colloid Interface Sci.* **1981**, *83*, 531.
(5) Shubin, V. E.; Kekicheff, P. *J. Colloid Interface Sci.* **1993**, *155*, 108.
(6) Raviv, U.; Laurat, P.; Klein, J. J. *Chem. Phys.* **2002**, *116*, 5167.
(7) Lyons, J. S.; Furlong, D. N.; Healy, T. W. *Aust. J. Chem.* **1981**, *34*, 1177.

10.1021/la802752g CCC: $40.75
Published on Web 01/02/2009

complex dynamic interactions occurring at the mica/solution interface.

Scales et al.[8] also reported zeta potential data based on streaming potential measurements in chloride salts of lithium, sodium, potassium, and cesium. Varying the pH from 3 to 10 in a background of 1 mM KCl, they found zeta potentials increased from approximately −35 to −80 mV for KCl. Similarly, they reported values of zeta potential ranging from −120 to −50 mV at a pH of 5.8 as the KCl concentration increased from less than 0.1 mM to approximately 10 mM. Nishimura et al.,[9] however, reported zeta potential data of "freshly cleaved mica" ranging from −95 mV at pH 4 to −140 mV at pH 10. They noted the difference between their results and the data of Scales, and the closer proximity to the results of Shubin and Kekicheff,[5] but could not resolve the discrepancy other than to point back to the large variations observed in mica from the beginning.[2]

Prior Modeling of the Mica/Solution Interface. Modeling the interaction of mica with aqueous solution rests on adsorption/desorption or ion exchange modeling and the finding of Goulding[10] that mica, unlike many other clay surfaces, has only one type of surface exchange site. Pashley[3,4] wrote adsorption/desorption reactions for the interaction of ions with mica and invoked an ion size argument. Scales et al.[8] used Yates's[11] triple layer model to fit zeta potential data as a function of salt concentration for Cs, K, Na, and Li electrolyte solutions in part by specifying the outer capacitance C_2 and the inner capacitance C_1 of the compact layer. This procedure successfully correlated both the charge and potential behavior of the mica/solution interface at pH 5.8, and it is equally valid to using ion size.

Summary and Present Work. The zeta potential of sheet mica, which one might expect to be reproducible, varies widely in published reports. The equilibrium constants for the adsorption of species on mica reflect that variability. Also, the model of Scales et al.[8] agreed well with data where the salt concentration was varied at a pH of 5.8, but it did not perform well as a function of pH. The scientific importance of mica, combined with the variability of results in the literature and the advent of a new apparatus,[12] motivated this investigation of the early transient response of mica.

Most experiments and theory concerning the zeta potential of mica have probed its state after periods ranging from hours to days; investigators did not address experimentally or theoretically the surface reactions occurring in much shorter time scales, in part because the means did not exist. The hypothesis of the present work was that observation of the transient behavior of zeta potential in the first minute after immersion can provide new perspective on the interaction of mica with aqueous solutions. We report measurements of the zeta potential of mica, acquired with the aid of a rotating disk, within seconds after cleaving and immersion. We also present a reaction kinetic model for interpreting the data and a compact equation that governs the zeta potential of sheet mica from pH 4 to 10 at arbitrary concentrations of KCl. The result is much simpler than was possible with prior models.

A dynamic model (dynamic charging model or DCM) of the interaction of freshly cleaved mica (FCM) with aqueous mixtures of HCl, KCl, and KOH is proposed. Figure 1 is a schematic of mica before and after immersion of FCM in solution. Before immersion, a surface concentration of lattice potassium ions S_L

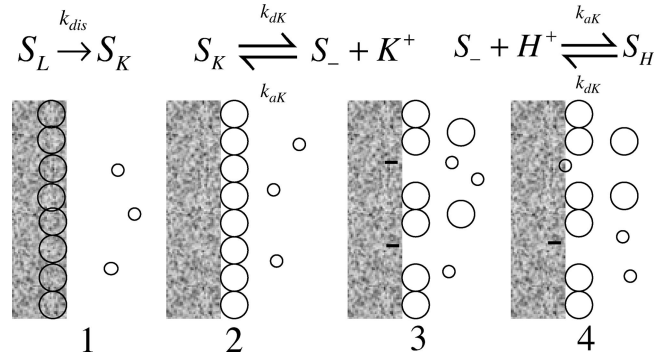

Figure 1. Schematic drawing of the dynamic charging model. The large and small circles represent potassium ions and protons, respectively. 1 → 2: Lattice potassium ion becomes adsorbed potassium ion. 2 → 3: Adsorbed potassium ion desorbs and equilibrates. 3 → 4: A proton adsorbs onto the mica and equilibrates.

exactly balances the negative charge associated with the mica lattice. Since the area per unit cell, N_s, is 0.458 nm^2,[8] the initial value of S_L, S_{L0}, is known. A single-site binding basis for the mica/solution interface was assumed because aging effects are minimal in the pH range investigated as per the study of Lyons et al.[7] The potassium atoms present at the surface of freshly cleaved mica progress from the lattice to their positions at the inner Helmholtz plane (IHP) and begin desorbing from the IHP as they become solvated. This desorption proceeds until adsorption of potassium ion from solution balances it. Protons from solution adsorb to the interface until adsorption balances desorption. Unlike the three-layer equilibrium model,[8,11] the DCM does not require specification of the location of either the protons or the adsorbed metal cations; it captures the phenomena with fewer unknown parameters.

As the potassium ions and protons change their position, co-ions and counterions from the solution move toward or away from the surface to provide shielding charge. The electrical double layer, forming in microseconds, comprises an outer diffuse charge region and an inner compact charge region. The DCM assumes the Gouy−Chapman−Stern−Graham (GCSG) description of the inner region of the electrical double layer and a Poisson−Boltzmann dependence of concentration in the diffuse layer. The diffuse part of the double layer is assumed to be in a quasi-equilibrium state at all times.

Theory

Five surface reactions were envisioned with their forward and backward rate constants. The first reaction is the irreversible promotion of potassium ion from the FCM surface to the IHP.

$$S_L \xrightarrow{k_{dis}} S_K \qquad \text{(I)}$$

S_L and S_K are the surface concentrations of lattice potassium and adsorbed potassium, respectively. Reaction I represents the progress of potassium ions from being an integral part of the mica lattice to their occupation of sites at the IHP. Reactions II and III represent the adsorption/desorption reactions of potassium ion and protons, respectively.

$$S_- + K^+ \underset{k_{dK}}{\overset{k_{aK}}{\rightleftharpoons}} S_K \qquad \text{(II)}$$

$$S_- + H^+ \underset{k_{dK}}{\overset{k_{aK}}{\rightleftharpoons}} S_H \qquad \text{(III)}$$

Here, S_- is the net surface concentration of negative charge balanced by the diffuse layer charge. Equation 1, based on

(8) Scales, P. J.; Grieser, F.; Healy, T. W. *Langmuir* **1990**, *6*, 582.
(9) Nishimura, S.; Scales, P. J.; Tateyama, H.; Tsunematsu, K.; Healy, T. W. *Langmuir* **1995**, *11*, 291.
(10) Goulding, K. W. T. *J. Colloid Interface Sci.* **1980**, *78*, 15.
(11) Yates, D. *Trans. Faraday Soc.* **1974**, *70*, 1807.
(12) Sides, P. J.; Newman, J.; Hoggard, J. D.; Prieve, D. C. *Langmuir* **2006**, *22*, 9765.

reaction I, governs the rate of progress of lattice potassium to the IHP.

$$\frac{dS_L}{dt} = -k_{dis}S_L \quad (1)$$

Equation 2 governs the rate at which singly charged negative sites S_- appear or vanish as adsorption and desorption proceed.

$$\frac{dS_-}{dt} = -k_{aK}S_-[K^+]_b e^{-\bar{\zeta}} + k_{dK}S_K - k_{aH}S_-[H^+]_b e^{-\bar{\zeta}} + k_{dH}S_H \quad (2)$$

Here, S_K and S_H are the surface concentration of sites bound with potassium ions and protons, respectively. Also, $\bar{\zeta}$ is defined as $e\zeta/k_BT$ with e, k_B, and T indicating the charge on an electron, Boltzmann's constant, and temperature, respectively. The reaction rate constants k_{aK}, k_{dK}, k_{aH}, and k_{dH} for adsorption of potassium ions, desorption of potassium ions, adsorption of protons, and desorption of protons, respectively, are unknown parameters. The exponential functions correct the bulk concentrations, for example, $[H^+]_b$, to the values for potassium ions and protons at the inner limit of the diffuse double layer. We have assumed that the zeta potential and the potential at the OHP are identical, which should be a good approximation for a smooth surface such as mica. A key point of the DCM is manifest in eq 2; the capacitances of the inner and outer regions of the compact layer, a feature of the three-layer model,[8,11] do not appear in this kinetic treatment. Equation 3 governs the rate at which potassium ions appear or vanish at the IHP.

$$\frac{dS_K}{dt} = k_{aK}S_-[K^+]_b e^{-\bar{\zeta}} - k_{dK}S_K + k_{dis}S_L \quad (3)$$

Equations 1−3 contain five variables and five parameters. A site balance on the mica surface provides a fourth equation.

$$N_s = S_- + S_K + S_H + S_L \quad (4)$$

N_s is the number of ionizable sites per unit area, taken for mica as $2.18 \times 10^{18}/m^2$.[8] The relationship between the surface charge density and the zeta potential provides one more constraint on the system:

$$S_- = -\frac{2\varepsilon k_B T}{e^2\lambda}\sinh\left(\frac{\bar{\zeta}}{2}\right) \quad (5)$$

where λ is the Debye length.

The assumptions made to this point are (1) the equivalence of zeta potential and the potential at the OHP, (2) single-site binding, and (3) the irreversibility of reaction I. Equation 1 can be integrated directly to give

$$S_L = S_{LO}e^{-k_{dis}t} \quad (6)$$

where S_{LO} equals N_s. The DCM for mica in contact with solutions of HCl, KCl, and KOH includes five unknown reaction rate parameters that might be fast or slow; experiments must provide guidance going forward. The objective of this work is to determine as many of the values of the rate constants as necessary to describe the behavior of mica observable in experiments.

Experimental Section

The experiments employed an advance in the instrumentation for zeta potential measurement of planar surfaces, the rotating disk, that uses axisymmetrical flow to engender streaming potential in its vicinity.[12] A schematic of the approach appears in Figure 2 showing the disk sample, a spindle with motor, and the placement of the sensors that detect streaming potential near the disk. When the disk is rotated, the two sensors measure a difference of streaming potential. One converts streaming potential to zeta potential with the aid of eq 7.

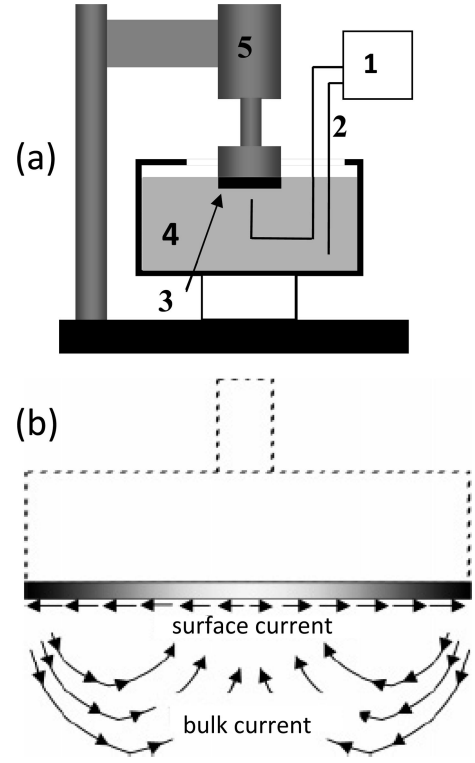

Figure 2. Schematic of the rotating disk apparatus. (a) A motor (5) spins a sample (3) immersed in liquid (4). The voltmeter (1) records the streaming potential difference reported by Ag/AgCl reference electrodes (2). (b) Surface current flows radially outward along the mica; the surface current becomes bulk (ohmic) current at the disk periphery in order to flow back to the disk.

$$\zeta(\bar{z}) = \frac{1.96\phi_s\kappa}{a\varepsilon\left(\sqrt{\frac{\Omega^3}{\nu}}\right)\left[\frac{1-2\bar{z}\sqrt{1+\bar{z}^2}+2\bar{z}^2}{\sqrt{1+\bar{z}^2}}\right]} \quad \text{where} \quad \bar{z} \equiv z/a \quad (7)$$

The symbols a, ϕ_s, Ω, ν, z, and ζ represent the disk radius, the measured streaming potential, disk rotation rate, kinematic viscosity, axial distance from the disk, and zeta potential, respectively. The distance z denotes the gap between the disk and a Ag/AgCl reference electrode located on the axis of the disk.[12] A precision positioning system supporting the cell of Figure 2a is used to place the sensor on the axis at a known z, in this case 1 mm.

The normal operating mode of the rotating disk involves modulation of the rotation rate sinusoidally at 0.2 Hz between zero and 4000 rpm for 1, 3, or 10 cycles during which the streaming potential is measured continually. Assuming quasi-steady operation, one fits the measured streaming potential to eq 7 as a function of time, with the only fitting parameter being the zeta potential. The time between immersion and the first data point is about 30 s, and data points accumulate at a rate of 1 point every 10 s, every 30 s, or every 60 s thereafter, depending on the number of cycles specified. This method limits the earliest meaningful data to about 30 s from immersion. Alternatively, we imposed a constant rotation rate and measured the streaming potential every 55 ms for approximately 1 min. The time between immersion and the start of sampling was the time required to position the sample; acquiring meaningful data within 10 s after immersion was typical for this technique.

Solutions were freshly made from reagent potassium chloride or potassium hydroxide dissolved in water from a Millipore Elix 3

reverse osmosis system followed by a four-barrel water polisher. In these cases, the concentrations ranged from 0.03 to 1.5 mM. In the case where no salt was added, the water was allowed to equilibrate with atmospheric carbon dioxide until the pH settled to a steady value, near 5.6, which occurred over a few minutes. The conductivity in the dynamic measurements was approximately 1 μS/cm. (One of the attributes of the rotating disk is that surface conductivity is not a problem because the large open domain of electrolyte adjacent to the sample invites the surface current to return through the bulk solution and not the diffuse layer even at low conductivity.) Where other solutions were tried, the salt or base was added to water already in the cell. A thermoelectric stage maintained the temperature at 25 °C. A sample was immersed after the temperature, solution conductivity, and pH were stable.

A mica disk 25.4 mm in diameter (SPI Supplies) was affixed with paraffin to a cylindrical sample support. In each experiment, a layer of mica was peeled from the disk on the sample support and the cylinder was then immediately screwed onto the spindle. The sample was on the spindle and ready for immersion approximately 20 s from the instant of cleaving. There is evidence that this length of time is well within the several minutes over which observable surface features associated with potassium ions vanish after cleaving in air.[13] For the most rapid determinations, the mica was cleaved, positioned above the solution, and rotated at 2000 rpm. After initiation of data acquisition, the mica was immersed and positioned 1 mm from the sensor on the axis. A total of 1000 measurements of potential difference between the reference electrodes of Figure 2 were acquired in 55 s. For experiments with durations on the order of minutes, the normal procedure, involving modulation of the rotation rate, was used.

Results

Streaming Potential near Muscovite Mica in the Absence of Bulk Potassium Ion. We employed the constant rotation rate approach to explore the relatively early behavior of mica in a solution where the pH was 5.6 and no potassium ion had been added. The streaming potential of one experiment, in terms of measured potential, appears in Figure 3a. The zero values at the earliest times correspond to the electrode spinning above the solution. The measured potential decreases as the spinning sample is immersed and lowered toward the reference electrode on the axis; conveniently, the sharp change of measured potential marks the zero of immersion time. Approximately 12 s after immersion, the sample was in position and meaningful streaming potential data were acquired. After elimination of the data before the sample was in the desired position, and after conversion of the streaming potential data to zeta potential with the aid of eq 7, the raw results of Figure 3a became the zeta potential data in Figure 3b. A clear transient was obtained; the zeta potential varied from −215 mV at 5 s after immersion to −170 mV at 50 s after immersion. The results of Figure 3b are mildly paradoxical. The initial zeta potential of FCM must have been zero because the mica was initially neutral; one might expect a monotonic variation from zero to a negative steady value. The direction of variation of zeta potential in these experiments, however, was from more negative to less negative, that is, opposite. This experiment was repeated three times for three freshly cleaved samples, and then the solution was discarded and replaced twice more. A total of nine otherwise equivalent experiments were performed; the pattern of Figure 3 was found in each case.

Streaming Potential at Higher pH in the Presence of Potassium Ion. We attempted similar experiments at higher pH and KCl concentrations. The measured zeta potentials of three experiments appear in Figure 4, plotted on the same linear scale as the data of Figure 3b. Figure 4 shows that the zeta potential of mica arrives at a steady charged state in fewer than 5 s in KCl solution at pH 9. The transition that mica undergoes in the first minute in these solutions is not resolvable. We then used the rotation rate modulation method to obtain equilibrium data for a variety of solutions, as shown in Figure 5. The zeta potentials in these solutions reached a steady value quickly, as shown in Figure 4, and maintained their values over minutes, as shown in Figure 5.

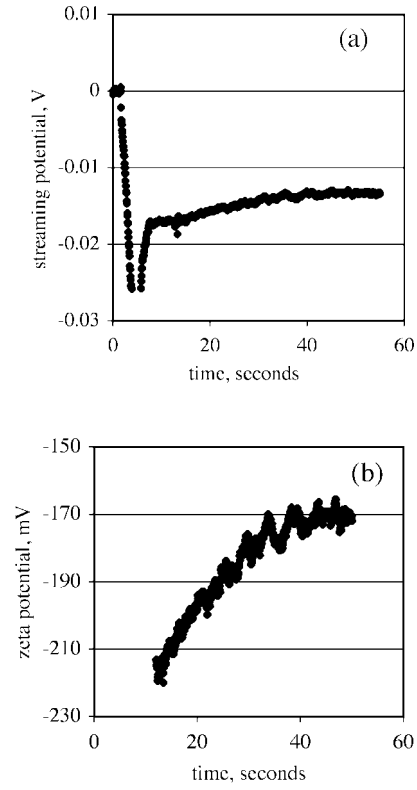

Figure 3. (a) Streaming potential data measured near a mica disk rotating at constant speed in water at pH 5.6. (b) Zeta potential calculated by eq 7 from the streaming potential shown in (a) after eliminating data acquired during positioning of the sample. Zeta potentials are quite negative in part because the Debye length is large at the low ionic strength of the experiment (no added salt).

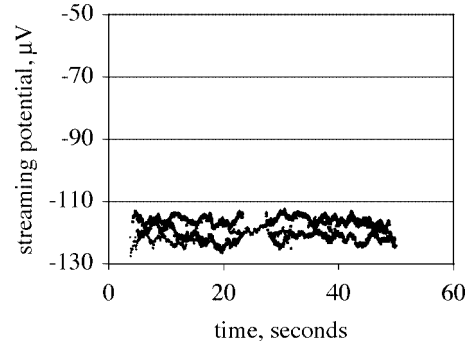

Figure 4. Streaming potential data acquired from three experiments involving FCM disks rotating at constant speed in a solution of KCl and KOH (50 μS/cm, pH 9). By comparison to Figure 3b, no transient was observed.

Titration of Mica. In a third set of experiments, mica was cleaved and titrated in 1 mM KCl from high pH to low pH. The mode of experimentation wherein the rotation rate was modulated was used for these experiments. The results of the titration appear

(13) Campbell, P.; Sinnamon, L.; Thompson, C.; Walmsley, D. *Surf. Sci.* **1998**, *410*, L768.

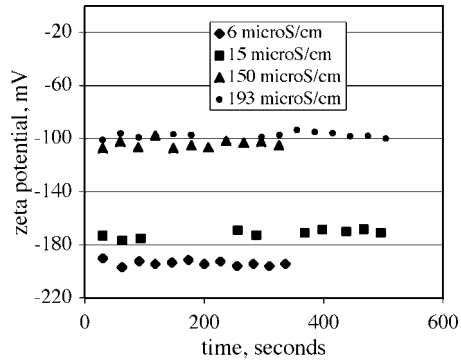

Figure 5. Zeta potential of FCM samples in various solutions. No transients were observed over minutes.

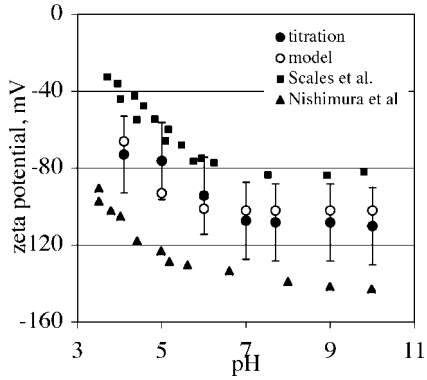

Figure 6. Titration data (●) acquired on FCM calculated from eq 19 and the parameters given in the text. Data of Scales et al.[8] (■) and Nishimura et al.[9] (▲).

in Figure 6 along with data reported by Scales et al.[8] and Nishimura et al.[9]

Discussion

The experiments revealed that the rotating disk can resolve dynamic charging at muscovite mica in the case of dilute acid solutions but the transient in alkaline salt solutions was not resolvable. The results at the two different pH values and salt concentrations can be used together, however, to quantify the charging of mica in KCl solutions within the help of the DCM.

The Zero Potassium Limit. Figure 3 demonstrated the dynamic response of mica to protons in the first minute after immersion in water equilibrated with atmospheric carbon dioxide; we adapted the general model described in the theory section to this circumstance. In the absence of bulk potassium ion, eqs 2 and 3 become

$$\frac{dS_-}{dt} = -k_{aH}S_-[H^+]_b e^{-\bar{\zeta}} + k_{dH}(N_s - S_- - S_K - S_L) + k_{dK}S_K \quad (8)$$

$$\frac{dS_K}{dt} = -k_{dK}S_K + k_{dis}S_L \quad (9)$$

Examination of the experimental data allowed simplifications of the theory. Using eq 5, we represented the data of Figure 3b as surface charge density in Figure 7, where N_s normalizes the surface concentration of charged sites. The values of $\bar{S}_-$, the fractional coverage of charged sites, ranged from 0.025 to 0.01, approximately, which means that more than 97% of the desorption of potassium ions and adsorption of protons has occurred; the charged sites are 2.5% of the available sites at the earliest

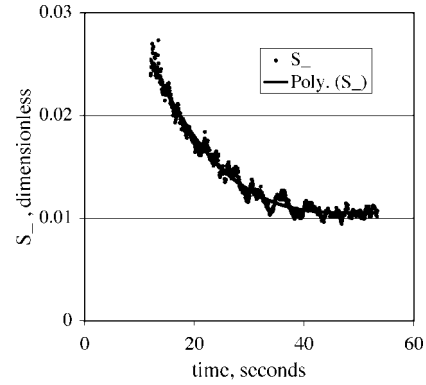

Figure 7. Zeta potentials of Figure 6 converted to site density $\bar{S}_-$ normalized by N_s. Equation 5 was used. The points are data, and the line is a polynomial fit to the data.

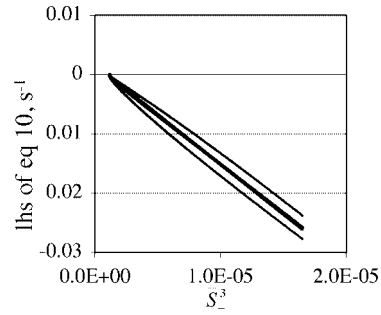

Figure 8. Data of Figure 7 plotted according to eq 10. The value of k_{dK} was adjusted until a linear representation was achieved. The curved lines above and below the fit of the data showed the effect of a 10% increase or decrease in the value of k_{dK}.

measurable state and 1% or less of the total sites after 60 s of exposure to the test solution. We made four approximations, therefore, with regard to eqs 8 and 9 *in the time frame of the experiment*: (1) k_{dis} is sufficiently large that the promotion of potassium ions from their positions on the mica surface to the IHP is fast and S_L is therefore zero. (2) The value of $\bar{S}_-$ is always negligible in comparison to N_s. (3) The desorption rate constant for protons k_{dH} is much smaller than the desorption rate constant for potassium ion k_{dK}. (4) The values of the zeta potentials of Figure 3a are sufficiently negative that the hyperbolic sine in eq 5 equals $(-e^{-\bar{\zeta}/2}/2)$ to a good approximation. Using these assumptions, integrating eq 9, and converting zeta potential to its corresponding charged site concentration $\bar{S}_-$ via eq 5, eq 8 became

$$\frac{d\bar{S}_-}{dt} - k_{dK}e^{-k_{dK}t} = -k_{aH}[H^+]_b\left(\frac{eF\lambda N_s}{\varepsilon RT}\right)^2 \bar{S}_-{}^3 + k_{dH} \quad (10)$$

Equation 10, the main result for the zero-potassium case, indicates that the difference between the overall rate of site binding and the rate of potassium desorption is proportional to the cube of the unbound site concentration in the time frame of these experiments.

Equation 10 suggests a way to obtain values for three of the four rate constants: k_{dK}, k_{aH}, and k_{dH}. Using the data of Figure 3b to find the derivative and cube function of eq 10, we tried values for the potassium desorption rate constant k_{dK} until a straight line was obtained. Figure 8, obtained by fitting the data of Figure 7 to a polynomial for smooth differentiation, shows an example of this process. The middle line represented the best fit to a straight line where the value of k_{dK} was 0.14 s^{-1}. The upper line and the lower line represented the function with a

value of $k_{dK} = 0.155$/s and 0.125/s, respectively, which shows that the method is sensitive to 10% changes of the optimum value. The slope of the line in Figure 8 was -1.68×10^3/s, and the intercept (k_{dH}) was 1.62×10^{-3}/s. Everything else in the coefficient of S_-^3 in eq 10 was known. Based on nine determinations of the slope and intercept, the average values of k_{aH}, k_{dH}, and k_{dK} were 45 L/s ± 15, 0.0014/s ± 0.0006, and 0.14/s ± 0.03, respectively. These values justified the assumption (no. 3 above) that k_{dK} is much larger than k_{dH}. When the proton adsorption/desorption rate constants were combined to form an equilibrium constant, the result was 4.64 ± 0.41, which falls between the value of 5.6 reported by Scales et al.[8] and the value 4.2 reported by Shubin and Kekicheff.[5]

The High pH Limit. At high pH, the DCM becomes a single ordinary differential equation based on combining eqs 2 and 4 with neglect of S_L as previously argued.

$$\frac{dS_-}{dt} = -k_{aK} S_- [K^+]_b e^{-\bar{\zeta}} + k_{dK}(N_s - S_-) \qquad (11)$$

The experimental data of Figure 4 indicate that the transient in this case is shorter than a few seconds; even the faster of the two approaches described herein did not resolve any part of it. Putting the derivative of eq 11 equal to zero, one obtains

$$\frac{S_-[K^+]_b e^{-\bar{\zeta}}}{(N_s - S_-)} = \frac{k_{dK}}{k_{aK}} \qquad (12)$$

Substitution of eq 5, neglect of S_- in favor of N_s, expansion of the hyperbolic function, and rearrangement produces

$$\frac{-\varepsilon k_B T [K^+]_b}{e^2 \lambda N_s}\left(e^{-\frac{\bar{\zeta}}{2}} - e^{-\frac{3\bar{\zeta}}{2}}\right) = \frac{k_{dK}}{k_{aK}} \qquad (13)$$

The formula for the Debye length, when the salt concentration dominates the acid/base contribution to the ionic strength, simplifies to

$$\lambda \cong \sqrt{\frac{\varepsilon RT}{2F^2[K^+]_b}} \qquad (14)$$

Combination of eqs 13 and 14, with neglect of the smaller of the two exponentials, yields

$$\left(\frac{2\varepsilon k_B T N_{avo}}{e^2 N_s^2}\right)^{1/2} [K^+]_b^{3/2} e^{-\frac{3\bar{\zeta}}{2}} = \frac{k_{dk}}{k_{ak}} \qquad (15)$$

Taking the 2/3 power of both sides of the equation, one obtains eq 16 after a final rearrangement.

$$\bar{\zeta} = 2.303\log([K^+]_b) - \ln\left\{\left(\frac{k_{dK}}{k_{aK}}\right)^{2/3}\left(\frac{2\varepsilon k_B T N_{avo}}{e^2 N_s^2}\right)^{-1/3}\right\} \quad \text{where} \quad \bar{\zeta} \equiv \frac{e\zeta}{k_B T} \qquad (16)$$

Equation 16 reveals that the zeta potential is proportional to the logarithm of the potassium salt concentration; the slope should be 2.303, the factor converting the natural log scale to the base-10 scale. The steady state data shown in Figure 5 are replotted on a log scale in Figure 9. The slope is 2.25, near the value 2.30 expected on theoretical grounds; the constant on the rhs of eq 16 is the intercept having the value −4.08. Combination of the data of Figure 5 and eq 16 allows determination of the ratio of the adsorption and desorption rate coefficients for potassium ion; here, $k_{dK}/k_{aK} = 0.0024 \times 10^{-3}$/L. Combining this ratio with the value of k_{dK} determined earlier, 0.14/s, one finds that $k_{aK} =$ 58 L/s ± 5. The adsorption rate coefficients of potassium ion and protons are similar, but the proton desorption rate constant is 2 orders of magnitude lower than the corresponding value for the potassium ion.

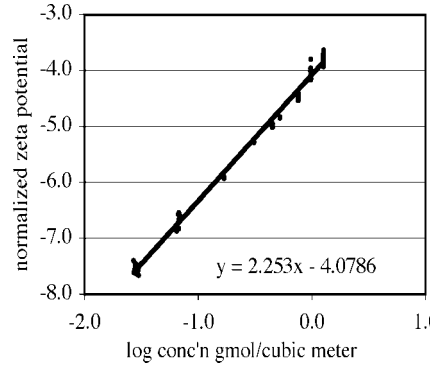

Figure 9. Zeta potential, normalized by *kT*/*e*, as a function of potassium ion concentration at pH 9. When plotted on a logarithmic scale, the result is linear with a slope close to 2.3. The concentration units for the potassium ion concentration are mol/m^3.

An Algebraic Model for the Equilibrium Zeta Potential of Mica. The method underlying eq 16 can be extended to generate a complete model for the HCl/KCl system in contact with mica within the limits of the two assumptions ($N_s \gg S_-$ and $\sinh x \approx -e^{-x}/2$ for large negative values of x) already employed. Inserting equilbrium expressions associated with reactions I and II into eq 4, and expressing the fraction of negatively charged sites as a function of zeta potential, one can write

$$1 = \frac{k_{aK}}{k_{dK}\bar{\lambda}}[K^+]_b e^{-\frac{3\bar{\zeta}}{2}} + \frac{k_{aH}}{k_{dH}\bar{\lambda}}[H^+]_b e^{-\frac{3\bar{\zeta}}{2}} \qquad (17)$$

Rearranging, one finds

$$\bar{\zeta} = \frac{2}{3}\ln\left(\frac{\frac{k_{aH}}{k_{dH}}[H^+]_b + \frac{k_{aK}}{k_{dK}}[K^+]_b}{\bar{\lambda}}\right) \quad \text{where} \quad \bar{\lambda} \equiv \frac{e^2\lambda N_s}{\varepsilon k_B T} \qquad (18)$$

Equation 18 shows the explicit dependence of zeta potential on the kinetic parameters and the cation concentrations. We tested this relationship against the titration data acquired with the rotating disk in the modulation mode of measurement. The favorable agreement between the model and experiment shown in Figure 6 indicates that the quantities derived from the kinetic measurements can be used to generate expected titration plots for mica.

Data from Scales et al.[8] and from Nishimura et al.[9] taken in similar conditions also appear in Figure 6. The differences among the sets of data might be understood in two ways. As noted in the Introduction, widely different values for the zeta potential of sheet mica have been found in surface force measurements.[2] Second, the methods and data of this work raise the question of what is meant by "freshly cleaved" mica. In the present case, FCM means that the experiment was carried out within 1 min after cleaving, while to Scales et al.[8] and Nishimura et al.[9] FCM meant mica cleaved and in contact with solution for much longer times. Another difference between the data sets, therefore, might be an issue of exposure time.

The form of eq 18 admits a possibility that bears on this question. Assume that one measures a value of zeta potential in a solution, changes the solution, and remeasures the zeta potential. The difference between the newer zeta potential and the original zeta potential is given by eq 19.

$$\zeta - \zeta_o = \frac{2kT}{3e} \ln\left[\frac{\frac{k_{aH}}{k_{dH}}[H^+]_b + \frac{k_{aK}}{k_{dK}}[K^+]_b}{\frac{k_{aH}}{k_{dH}}[H^+]_{bo} + \frac{k_{aK}}{k_{dK}}[K^+]_{bo}} \frac{\lambda_o}{\lambda}\right] \equiv \Delta\zeta \quad (19)$$

The subscript o denotes the initial state. Note that N_s cancels, which means that subtraction of the two zeta potentials eliminates the total number of ionizable sites from the difference $\Delta\zeta$ between the new zeta potential and the original zeta potential. This effect might be useful for analyzing data of minerals from repeated experiments where the variation from run to run or sample to sample introduces errors. Under this transformation, the starting state cancels and the zeta potential depends only on the intrinsic rate parameters and species concentrations. Replotting the data of Figure 6 according to eq 19 provides evidence supporting this approach (see Figure 10). Thus, mica might best be viewed as having a variable N_s from specimen to specimen but consistent intrinsic parameters characterizing its equilibria with ions.

Speculation about the Earliest Behavior of Mica. Having values for the reaction kinetic parameters allows a speculative calculation about the early charging behavior of mica. Solving eqs 8 and 9 with known kinetic parameters, with neglect of S_L, and with an initial condition, $\bar{S}_- = 0$, gives the result shown in Figure 11 without restrictive assumptions about the magnitude of zeta. Measured streaming potential data have been converted to fractional charged site concentration $\bar{S}_-$, and the values of k_{aH} and k_{dK} determined for that experiment are used in the calculation of $\bar{S}_-$ from the model. The model represents the data exceptionally well. Given the quality of the agreement in Figure 10 and the overall agreement between experiment and the model described in this contribution, we suggest that the behavior of the charged site concentration obeys the pattern shown in Figure 11. The charging process begins with desorption of potassium ions (S_K); while potassium ions are desorbing, protons (S_H) begin adsorbing. The consequence of the parallel progress of desorption and adsorption is a maximum in the charged site concentration (S_-) and an accompanying minimum of zeta potential, which explains

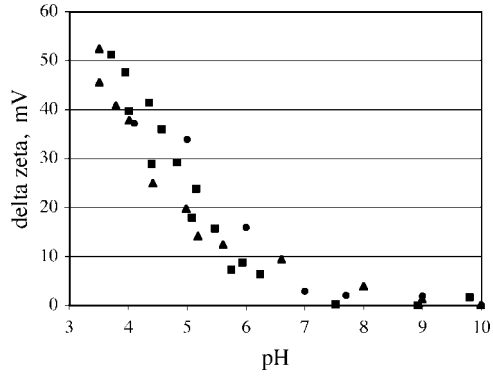

Figure 10. Data of Figure 6 rendered as $\Delta\zeta$ calculated by subtracting the zeta potential at pH 9 from each other measurement. (▲) Nishimura et al.,[9] (●) this work, (■) Scales et al.[8] Normalizing out the number of ionizable sites as per eq 19 reveals the intrinsic equilibria.

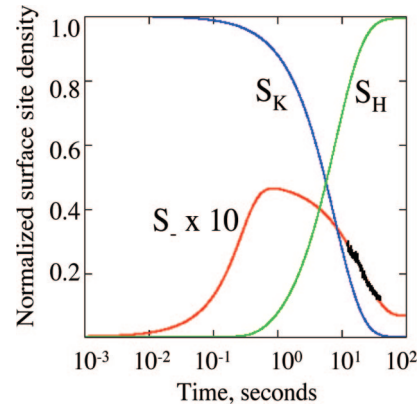

Figure 11. Plot of the charging process of mica in water at pH 5.6. Experimental data are the black points. The potassium ions desorb slightly faster than the protons adsorb until most of the potassium ions are gone, and then the protons adsorb faster. The changing relationship of the rates causes the maximum in the charged site concentration.

the previously cited paradoxical observation that the transient zeta potential of Figure 3b is increasing from more negative values to more positive values at the earliest recorded time, despite the fact that the initial condition on zeta potential must be zero. The initial rate of potassium desorption is high because the initial concentration of adsorbed potassium is high. The initial rate of proton adsorption is low because there are few charged sites available. Thus, the charged site concentration increases strongly from zero, rapidly giving a very negative zeta; when the rate of potassium desorption slows and the rate of proton adsorption increases, a maximum in the charged site concentration (hence a minimum of zeta potential) appears, as shown in Figure 11.

Conclusions

The main conclusions are that dynamics of charging of mica can be observed within the first minute after immersion in some cases, and that zeta potential data from the transient response of mica can be used along with appropriate theory to obtain meaningful rate parameters and equilibrium constants for mica in contact with aqueous solutions. This theory led to a general equation expressing the equilibrium zeta potential as a function of potassium ion and proton concentration. Furthermore, it was shown that a simple subtraction of zeta potentials within a given experiment cancels the effect of the original site density and brings disparate data into agreement. The result of the subtraction, $\Delta\zeta$, retains the influence of rate constants but eliminates dependence on the total ionizable site density of that particular sample, which eliminates a source of extrinsic error from the data.

Acknowledgment. The authors gratefully acknowledge the support of the National Science Foundation under Grant CTS 0521719 and the work of Melissa Bartel who acquired the titration data.

LA802752G